Trapping of electrons near chemisorbed hydrogen on graphene

J. A. Vergés* and P. L. de Andres
Instituto de Ciencia de Materiales de Madrid, CSIC, Cantoblanco, 28049 Madrid, Spain
(Received 22 May 2009; revised manuscript received 15 January 2010; published 18 February 2010)

Chemical adsorption of atomic hydrogen on a negatively charged single-layer graphene sheet has been analyzed with *ab initio* density-functional theory calculations. We have simulated both finite clusters and infinite periodic systems to investigate the effect of different ingredients of the theory, e.g., exchange and correlation potentials, basis sets, etc. Hydrogen's electron affinity dominates the energetic balance in the charged systems and the extra electron is predominantly attracted to a region nearby the chemisorbed atom. The main consequences are: (i) the cancellation of the unpaired spin resulting in a singlet ground state and (ii) a stronger interaction between hydrogen and the graphene sheet.

DOI: 10.1103/PhysRevB.81.075423 PACS number(s): 73.20.Hb, 68.43.Bc, 82.65.+r, 75.70.Rf

I. INTRODUCTION

Planar two-dimensional graphene has been considered to be a very promising new material since its preparation by Novoselov *et al.*[1] and Berger *et al.*[2] in 2004. Recent interest is focused on the appearance of magnetism around point defects in graphene[3] and the possibility of hydrogen storage.[4–7] A global understanding of the origin of magnetism in finite graphene systems is provided by Lieb's theorem on bipartite lattices.[8] Any unbalance between the numbers of sites belonging to each of the two sublattices gives rise to a magnetic ground state.[9] This result rests on the validity of a simple Hubbard Hamiltonian which certainly works for the semiquantitative description of the spin states of some polycyclic aromatic hydrocarbon molecules but not for the corresponding charged states.[10] The saturation of a carbon π electron by hydrogen is one of the simplest ways to change the balance between sublattice sites and, consequently, it produces spin polarization in the neighborhood. This provides an interesting link between hydrogenation and spin production that motivates this work. We shall demonstrate that the 1/2 spin originated by the presence of an isolated hydrogen atom on top of a carbon atom belonging to planar graphene can be quenched if an extra electron bounds to the defect. Numerical results obtained by *ab initio* open-shell density-functional theory (DFT) suggest that the complex defect is energetically favorable. A similar spin quenching phenomenon was discussed some years ago by Duplock *et al.*[11] for hydrogen near a Stone-Wales defect. These authors have shown that the spin-polarized ground state around chemisorbed hydrogen disappears in the presence of a Stone-Wales defect. In their interpretation, this result is probably due to the strong destruction of alternation near the defect that eliminates the tendency to antiferromagnetic order. In our case, however, we argue that the mere flow of charge is enough to heal the local unbalance between sublattices due to the existence of one chemisorbed hydrogen on an otherwise ideal graphene material.

The rest of the paper is organized as follows. The *ab initio* methods used in this work are presented in Sec. II followed by the discussion of our main numerical results. Final Sec. III just remarks our main message.

II. *AB INITIO* CALCULATIONS: METHODS AND RESULTS

Two planar carbon clusters with the structure of graphene have been chosen to calculate the energetics of hydrogen absorption both at the neutral state and when the system is electronically charged with an extra electron (anions). The first system is the well-known coronene polycyclic aromatic hydrocarbon (PAH) represented in Fig. 1 while the second one is a larger PAH obtained from coronene adding an extra shell of benzene rings. This system is referred as supercoronene in the literature. We notice that this larger PAH molecule has not yet been synthesized but nonetheless it provides a good theoretical benchmark for our purposes (Fig. 2 schematically shows one hydrogen chemisorbed on supercoronene). The ground state for both PAH's does not show spin polarization (total spin is zero). This is an important difference with our previous study of hydrogen chemisorption on graphene where spin one-half clusters were used to preserve the point symmetry and facilitate the computational effort.[5] In the present work, however, we focus on the description of spin polarization and we must start with an un-

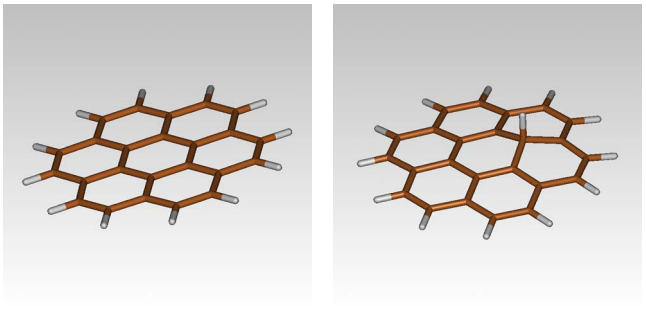

FIG. 1. (Color online) Left panel: schematic representation of a coronene molecule showing a honeycomb lattice inner structure saturated in the boundary by hydrogen atoms so the coordination of carbon atoms is preserved over the whole system. Right panel: an extra hydrogen atom is chemisorbed on top of a carbon atom belonging to the inner ring of coronene. Although the sp^2 to sp^3 reconstruction is only faintly visible in the figure, the C-H bonding distance and the details of the upward relaxation of C neighboring atoms coincide with those given in Ref. 5.

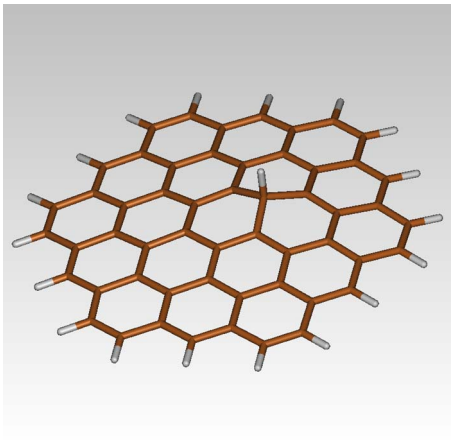

FIG. 2. (Color online) Hydrogen chemisorbed on supercoronene ($C_{54}H_{18}$).

polarized cluster to accurately simulate the graphene layer. Point symmetry is lost and computational load is larger. Nevertheless, we have checked that both structural and energetic results for chemisorbed H coincide with the values given in our previous work.[5]

Quantum-chemistry calculations have been done using the GAMESS program.[12] Several sets of Gaussian basis functions have been employed. Depending on the computational effort we have been able to assess the convergence of numerical results for some cases by comparing results obtained with bases of different sizes. For the largest systems, however, we have been forced to choose a minimal basis and convergence could only be assessed by reference to the smaller clusters. Specifically, we have always started by trying the so-called MIDI basis,[13] and when possible we have moved to a correlation consistent basis referred in the literature as cc-pVTZ (Ref. 14) (CCT within GAMESS and this paper) and a DFT adapted hierarchy of basis called PC*n*, where *n* indicates the level of polarization.[15] Our best results correspond to the larger PC*n* basis that we have been able to use in each case. Unrestricted Hartree Fock calculations have been intentionally avoided because total spin of the wave function is undefined in those cases. Therefore, HF calculations for an odd total number of electrons have been performed using the restricted-open-shell variant. All results presented in this work for clusters have been obtained using the Becke-Lee-Yang-Parr hybrid density-functional RB3LYP.[16]

Our choice of finite clusters of various sizes poses the question of to what extent results are affected by the particular boundary conditions imposed to solve the quantum problem for electrons. Therefore, we check by comparing with calculations performed on extended periodic models using periodic boundary conditions and a plane-waves basis. This model is setup so a single H atom is adsorbed on a 4×4 graphene supercell including 32 carbon atoms on a honeycomb lattice (see Fig. 6, $a=b=9.84$ Å, $c=23.4$ Å, $\alpha=\beta=90°$, and $\gamma=60°$). We use ultrasoft pseudopotentials,[17] an energy cutoff of 310 eV, and a Monkhrost-Pack mesh of $3\times3\times1$.[18] Actual calculations are performed with the CASTEP program allowing for spin polarization of the different electronic bands.[19,20] To describe the exchange and correlation potential we use the local-density approximation.[21] Forces and stresses on the system are converged to the usual thresholds (9×10^{-3} eV/Å and 0.01 GPa) and the total energy is minimized for the different systems. This procedure cannot provide an accurate description for the electron-affinity energy since the extra electron in the supercell is intentionally neutralized with a uniform positive background to subtract infinite contributions in the periodic system. This uniform background, however, has little effect on the spatial distribution of the electronic and spin densities, that can be analyzed with reasonable confidence.

Table I compiles the bulk of our quantum-chemistry results. Notice that together with the total energies needed to get chemisorption energies for hydrogen on graphene, we have computed the energies corresponding to systems charged with an extra electron (anions in the molecular case). Total spin of the ground state is given by the second column of the table. It can be seen that the $S=0$ value of the neutral molecules is recovered by the anions of the hydrogenated cases. Table II gives the electron affinities that are obtained

TABLE I. Total energies (in hartree) for atomic hydrogen and its anion, for coronene ($C_{24}H_{12}$) and coronene anion $(C_{24}H_{12})^-$ both ideal and with a chemisorbed H atom and for a larger cluster ($C_{54}H_{18}$) sometimes called supercoronene and its anion both planar and deformed by the presence of a chemisorbed H atom. Since results are given for two or more Gaussian basis sets some rough estimation of error is possible.

Cluster	Total spin	Energy(MIDI)	Energy(CCT)	Energy(PC2)	Energy(PC3)
H	$\frac{1}{2}$	−0.4953	−0.4988	−0.4990	−0.4991
H^-	0	−0.4602	−0.5035	−0.5177	−0.5254
$C_{24}H_{12}$	0	−915.9342	−921.6070	−921.6516	−921.6950
$(C_{24}H_{12})^-$	$\frac{1}{2}$	−915.9342	−921.6186	−921.6660	−921.7097
$C_{24}H_{13}$	$\frac{1}{2}$	−916.4438	−922.1269	−922.1723	
$(C_{24}H_{13})^-$	0	−916.4853	−922.1812	−922.2300	
$C_{54}H_{18}$	0	−2055.5931		−2068.3971	
$(C_{54}H_{18})^-$	$\frac{1}{2}$	−2055.6323		−2068.4469	
$C_{54}H_{19}$	$\frac{1}{2}$	−2056.1072		−2068.9095	
$(C_{54}H_{19})^-$	0	−2056.1868		−2068.9919	

TABLE II. Electron affinities of hydrogen, coronene, monohydrogenated coronene, supercoronene, and monohydrogenated supercoronene obtained from the results compiled in Table I. Energies are now given in electron volt.

Cluster	Energy(CCT)	Energy(PC2)	Energy(PC3)	Experimental
H	0.13	0.51	0.72	0.75[a]
$C_{24}H_{12}$	0.32	0.39	0.40	0.47[b]
$C_{24}H_{13}$	1.48	1.57		
$C_{54}H_{18}$	1.07[c]	1.35		
$C_{54}H_{19}$	2.17[c]	2.24		

[a]See, for example, http://www.chemicool.com/elements/hydrogen.html.
[b]The electron affinities of coronene and coronene dimer have been measured by Duncan *et al.* as reported in Ref. 23.
[c]This result corresponds to the small MIDI basis type of calculation that is described in Ref. 13.

from the results shown in Table I.[22] Nice convergence to the experimental electron affinity of hydrogen is observed in the first entry of the table. Results for larger clusters are limited by our computational means but nonetheless our results at the PC2 level are good enough to support our conclusions. A word of caution is in order here: although these results for the spin seem to fit nicely within a simple electron-counting scheme (i.e., zero spin for even number of electrons and net spin for odd number of electrons) this is not always true. In particular, we recall the case where two hydrogen atoms are adsorbed on the graphene layer: while adsorption of the two hydrogens in next-neighbor positions results in a ground state with no net spin, adsorption in next to next-neighbor sites results in a ground state with a net $S=2\mu_B$. This is related to the fact that graphene is a bipartite lattice, and it is in accordance to Lieb's theorem,[8] showing the limitations of simple electron-counting rules.

Let us briefly discuss the results given in Table II. The electron affinity of $C_{24}H_{13}$ cluster, i.e., the cluster with one hydrogen chemisorbed on top of one of the six carbon atoms on the inner ring of coronene (see, Fig. 1) is 1.18 eV larger than the electron affinity of coronene. Also, the value for $C_{54}H_{19}$, that is, H on top of supercoronene is 0.89 eV larger than the supercoronene electron affinity. Although, only two cluster sizes have been studied, it seems that the difference is approaching a limiting value close to the electron affinity of free hydrogen, that is, close to 0.75 eV. If this were the case, the extra charge would be attracted by hydrogen with a similar strength as in free space and the screening by the rest of π electrons of graphene would remain unnoticed. Nevertheless, we show later that only part of the extra charge remains close to the defect. Therefore, we assume that for an infinite system only a fraction of 0.75 eV proportional to the localized charge would remain.

There is an alternative elaboration of the results given in Table I focusing on the variation in the binding of a hydrogen atom on top of a charged surface compared to the binding by the neutral one. From this point of view, H binding energy increases from 0.59 to 1.77 eV on coronene and from 0.36 to 1.25 eV in supercoronene using PC2 values in Table I.[24] This means that the charged systems bind hydrogen about 1 eV stronger than the neutral ones. From this perspective, the larger values of the electron affinity obtained for hydrogenated clusters can be assigned to a stronger hydrogen binding to graphene.

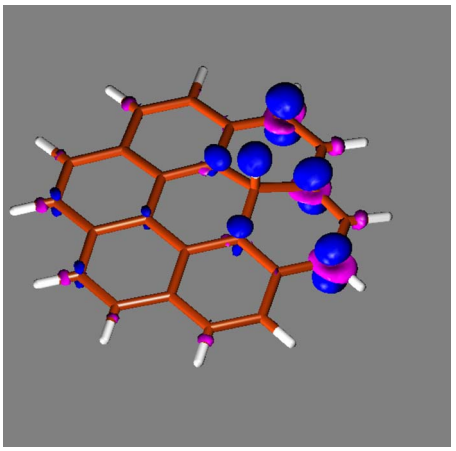

FIG. 3. (Color online) Charge difference between the anion of coronene and the neutral molecule. Density isocontours of $\pm 0.002\ e/\text{Å}^3$ are represented.

The relative facility to move charge across the overall system implied by the semimetallic character of graphene and our results in Table II point toward the formation of a complex point defect with an extra electron in the neighborhood of the chemisorbed hydrogen atom. This picture is further supported by the spatial distribution of this extra electron in the studied clusters as it is shown in Figs. 3 and 4. Charge densities obtained with PC2 Gaussian basis for coronene anion and neutral coronene have been subtracted in Fig. 3 using the MOLDEN package.[25] The same difference for supercoronene is given in Fig. 4. In both cases, the charge around "on top" H is similar to the extra charge of the H anion. On the other hand, the spreading positive and negative densities are similar but not equal in coronene and supercoronene. A closer inspection reveals that the extra electron is occupying the partially occupied highest occupied molecu-

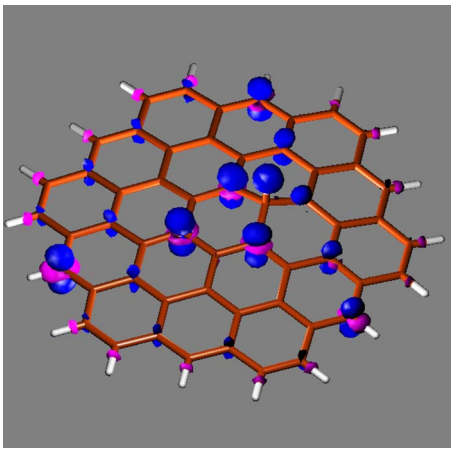

FIG. 4. (Color online) Charge difference between the anion of supercoronene and the neutral molecule. Density isocontours of $\pm 0.002\ e/\text{Å}^3$ are represented.

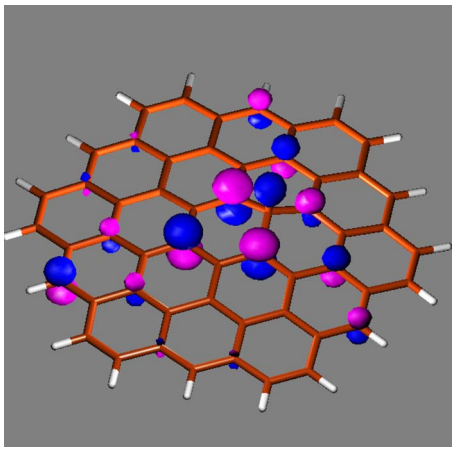

FIG. 5. (Color online) HOMO orbital of supercoronene. Isocontours of ± 0.05 Å^{-3} are represented.

lar orbital (HOMO) level of the corresponding neutral clusters. Figure 5 gives a picture of the HOMO orbital of H on supercoronene that nicely explains the charge difference previously shown in Fig. 4. It is interesting to notice, however, that although the extra charge clusters around the adsorbate, it is partly delocalized as it is expected from quantum-mechanics principles. In fact, from independent tight-binding calculations in periodic systems we do not find a true *exponential* localization around the defect (see appendix). On the contrary, a percentage of the charge is extended all over the system (e.g., see Fig. 4). However, as our detailed quantum-mechanical calculations show, the net effect of the localized part is enough to quench the spin.

Our *ab initio* results on periodic extended systems fully support the interpretation given in the previous paragraph. We observe in Fig. 6 how the extra charge is accumulated around the adsorbed H. In this case, bonding charges for the neutral and charged supercells are depicted in the right and left panels of the figure, respectively. Bonding charges are defined as density charge differences between the whole system and conveniently defined fragments. In our case, hydrogen atom is one fragment while the graphene 4×4 supercell is the second one. The right difference integrates to one electron charge since the whole system is charged while the fragments are neutral. We notice that a small part of the extra electron is on carbon atoms while an important part attaches to hydrogen (the violet negative density in the right panel does not appears in the left panel meaning a positive contribution to the extra charge in the left panel). The same picture is extracted from a Mulliken analysis of populations around different atoms. In the neutral system, charge flows upon adsorption from hydrogen to graphene, so approximately $-0.63e$ is located around hydrogen while the transferred charge resides mostly around the closest carbon behind hydrogen ($-0.33e$). On the other hand, in the charged system we find $-1.42e$ around hydrogen, while the carbon behind keeps nearly the same occupation ($-0.34e$) and the rest of the charge is distributed over nearest neighbors and next-nearest neighbors. Therefore, about 80% of the extra electron is located near the chemisorbed hydrogen. Along the same line, the H-C bond population analysis is about three times larger for the anion, although the bond length is nearly not affected. Finally, integration of the spin density and the absolute value of the spin density over the simulation cell give further support for this picture. In the neutral system these values amount to $0.4\mu_B$ and $0.5\mu_B$, respectively, while in the charged one decrease to values $4\times10^{-6}\mu_B$ and $5\times10^{-4}\mu_B$, respectively. Therefore, the accumulation of charge around the adsorbed H and the C nearest and next-nearest neighbors plays the role to cancel the extra spin polarization brought by the adsorption of H on the clean graphene layer in accordance with the results obtained on finite clusters.

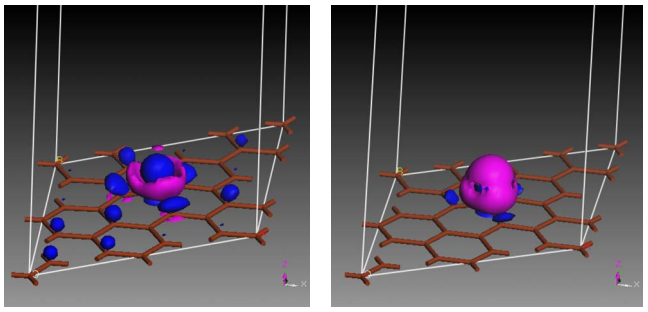

(a) (b)

FIG. 6. (Color online) A 4×4 graphene supercell with a single adsorbed H atom showing the bonding charge density first for the system with one extra electron (left panel) and, second, for the neutral system (right panel). Density isocontours of ±0.04 e/Å^3 are given (blue and violet, respectively). The accumulation of charge near H is seen to be the origin for the cancellation of the extra spin.

There is a subtle chemical argument that helps the understanding of our numerical results. In Ref. 26, trivalent carbon atoms with an unpaired electron were unraveled in the studied geometry of carbon tetrapod. These carbon radicals were stabilized by steric protection giving rise to unpaired localized electrons that polarize the carbon neighborhood and explain the appearance of magnetism in pure organic systems. The original paradigm is tryphenilmethyl, synthesized by Gomberg in 1900,[27] where a trivalent carbon atom is stabilized by three bonds to benzene rings impeding the reaction with a similar molecule. Nevertheless, the anion of tryphenilmethyl reacts with a proton to form a strong C-H bond (heat of reaction amounts to 15.65 eV per molecule)

$$C_{19}H_{15}^{-} + H^{+} \rightarrow C_{19}H_{16},$$

producing a neutral nonmagnetic molecule resembling the clusters that we have studied here.[28] Both the number of H atoms and electrons are even allowing an easy shell closing and stabilization of the resulting molecule. We can adapt the underlying chemistry of these phenomena to the binding of H on graphene using the following argument: it can be thought that when H forms a covalent bond with a C atom of graphene the two binding electrons are paired but additionally and due to the particular topology of graphene lattice one π electron becomes unpaired and, therefore, spin polarized. Since there is no steric protection around the defect (a kind of radical) any free electron of the system will flow into

the defect to restore the equilibrium between sublattices. Consequently, spin polarization around chemisorbed hydrogen disappears. This qualitative argument is fully supported by our total-energy calculations showing a gain in potential energy following the spin neutralization (remember that the binding energy of H increases about 1 eV for the charged system).

III. CONCLUDING REMARKS

From a detailed analysis based in first-principles DFT calculations we find that in the presence of an extra electron chemisorbed H plays to keep most of the extra charge in its vicinity. The electron affinities computed on finite cluster models seem to converge to a value that is somewhat smaller than the free atomic hydrogen value of 0.75 eV. Our calculations suggest that being graphene a semimetal with zero density of states at the Fermi energy, screening of Coulomb interactions by the π-electrons liquid is weak and allows the electron flow to sites where H is chemisorbed, forming a complex point defect. Accumulation of extra charge around the defect, otherwise giving rise to spin polarization, works to quench it. We suggest that this physical effect is behind the difficulties to observe magnetism in graphene-derived systems.

ACKNOWLEDGMENTS

Financial support by the Spanish MICINN (Grants No. MAT2006-03741, No. MAT2008-1497, No. FIS2009-08744, and No. CSD2007-41) is gratefully acknowledged.

APPENDIX: A TIGHT-BINDING CALCULATION

A tight-binding model including carbon π orbitals and hydrogen 1*s* orbital allows a straightforward although approximate solution of the topic covered in this paper. Since larger sizes can be studied, qualitative conclusions on the scaling behavior of the charged system can be obtained. This calculation fully supports our arguments based on the computationally demanding *ab initio* study done in the main part of the paper for smaller systems. Although total energies are not attainable by the method, both the density of states and the charge distribution of an extra electron suggest the stability of a charged hydrogen atom bonded to graphene.

The p_z-p_z hopping term of the Hamiltonian is −2.71 eV. Comparing the ionization energy of H (13.60 eV) to the value for the methyl radical (9.84 eV) we take the H level relative to the π one as −3.76 eV. This is justified because of the similarity between graphene and methyl radical p_z orbital. For the C-H coupling we have taken −5.39 eV based on a simple scaling argument. A standard supercell procedure and a carefully BZ integration have been used to get accurate density of states and local charge magnitudes. Although very large supercells have been explored (50×50), we will give here results for a 10×10 system because it shows almost converged results that are better depicted.

Figure 7 shows the total density of states per spin of the supercell. It integrates to 402 (total number of states of the cell) and shows two salient features: (i) a deep level below

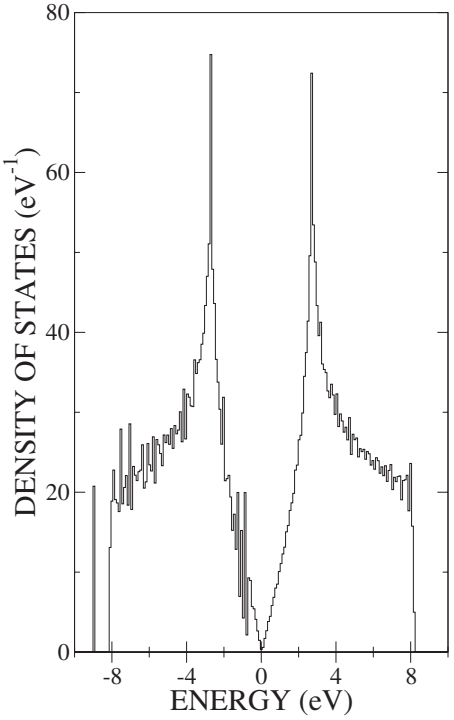

FIG. 7. Total density of states of a 10×10 supercell calculation of a graphene layer containing one hydrogen atom forming a strong covalent bond with one of the carbon atoms of the layer. Its integration up the Dirac point at $E=0$ gives one extra electron above half-filling.

the valence-band describing the bonding C-H orbital and (ii) strongly perturbed values below Dirac's point energy (0 in the clean system). Nevertheless, the most interesting feature relative to this density of states (DOS) is that it integrates to 202 up to the Dirac energy ($E=0$), i.e., the complete occupation of the valence band describes one extra electron above half-filling which is only 201 (200 electrons corresponding

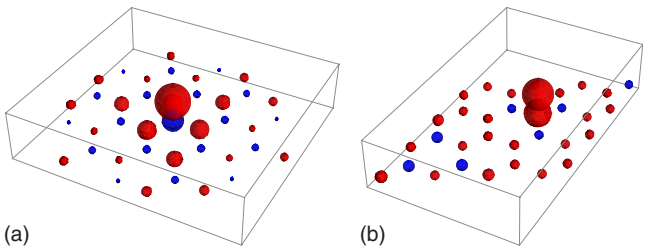

FIG. 8. (Color online) Spatial distribution of the extra electron charging the hydrogenated supercell. The sphere volume is proportional to the extra number of electrons of the corresponding atom, red if positive and blue if negative. The relevant part of the tight-binding results obtained for a 10×10 supercell calculation is given in the left panel whereas *ab initio* results for the 4×4 supercell are shown in the right panel. Last values are based on Mulliken populations. Overall trends coincide but details differ: both bonded H and C atoms get extra population when analyzed by the Materials Studio (CASTEP) package but not for the semiempirical model, for example. Although this representation of the extra charge cannot be directly compared with isocountours shown in Figs. 3 and 4, the overall distribution looks similar.

to the 200 π orbitals of C atoms plus one electron contributed by H). This means that when the Fermi level coincides with the Dirac point of graphene, a region with a quimisorbed H atom becomes charged by an extra electron. Since the full occupancy of the valence band can be thought as closing electronic shells, some stabilization of the system can be inferred from this property of the DOS.

The ideas suggested by the DOS are confirmed by the spatial distribution of the electronic charge induced by the addition of an extra electron to the system. Figure 8 (left panel) has been obtained subtracting the background charge of one electron per site from a 10×10 supercell with an additional electron. The resulting distribution can be compared with the corresponding variations in Mulliken populations of our *ab initio* results (right panel). It shows that an important amount of charge directly resides on the hydrogen atom although the underlying carbon atom somewhat reduces the net value on the binding site in the empirical model results. Yet another important part of the electron lies close to this site whereas the rest is spread over the whole supercell. The most intriguing characteristic of the charge distribution is its dual nature of localized around the defect and extended over the whole system.[29] In any case, a tight-binding model with a minimum number of orbitals reinforces our idea signaling the tendency of electrons to remain in the neighborhood of bounded hydrogen.

*jav@icmm.csic.es

[1] K. S. Novoselov, A. K. Geim, S. V. Morozov, D. Jiang, Y. Zhang, S. V. Dubonos, I. V. Grigorieva, and A. A. Firsov, Science **306**, 666 (2004).

[2] C. Berger, Z. Song, T. Li, X. Li, A. Y. Ogbazghi, R. Feng, Z. Dai, A. N. Marchenkov, E. H. Conrad, P. N. First, and W. A. de Heer, J. Phys. Chem. B **108**, 19912 (2004).

[3] P. Esquinazi, A. Setzer, R. Höhne, C. Semmelhack, Y. Kopelevich, D. Spemann, T. Butz, B. Kohlstrunk, and M. Lösche, Phys. Rev. B **66**, 024429 (2002); K. Kusakabe and M. Maruyama, *ibid.* **67**, 092406 (2003); A. N. Andriotis, M. Menon, R. M. Sheetz, and L. Chernozatonskii, Phys. Rev. Lett. **90**, 026801 (2003); N. Park, M. Yoon, S. Berber, J. Ihm, E. Osawa, and D. Tomanek, *ibid.* **91**, 237204 (2003); P. O. Lehtinen, A. S. Foster, Y. Ma, A. V. Krasheninnikov, and R. M. Nieminen, *ibid.* **93**, 187202 (2004); Y.-W. Son, M. L. Cohen, and S. G. Louie, Nature (London) **444**, 347 (2006).

[4] Y. Miura, H. Kasai, W. A. Diño, H. Nakanishi, and T. Sugimoto, J. Phys. Soc. Jpn. **72**, 995 (2003).

[5] P. L. de Andres and J. A. Vergés, Appl. Phys. Lett. **93**, 171915 (2008).

[6] D. W. Boukhvalov, M. I. Katsnelson, and A. I. Lichtenstein, Phys. Rev. B **77**, 035427 (2008).

[7] D. C. Elias, R. R. Nair, T. M. G. Mohiuddin, S. V. Morozov, P. Blake, M. P. Halsall, A. C. Ferrari, D. W. Boukhvalov, M. I. Katsnelson, A. K. Geim, and K. S. Novoselov, Science **323**, 610 (2009).

[8] E. H. Lieb, Phys. Rev. Lett. **62**, 1201 (1989).

[9] A summary of this explanation was recently published by J. Fernández-Rossier and J. J. Palacios, Phys. Rev. Lett. **99**, 177204 (2007).

[10] J. A. Vergés, G. Chiappe, E. Louis, L. Pastor-Abia, and E. San-Fabián, Phys. Rev. B **79**, 094403 (2009).

[11] E. J. Duplock, M. Scheffler, and P. J. D. Lindan, Phys. Rev. Lett. **92**, 225502 (2004).

[12] M. W. Schmidt, K. K. Baldridge, J. A. Boatz, S. T. Elbert, M. S. Gordon, J. H. Jensen, S. Koseki, N. Matsunaga, K. A. Nguyen, S. J. Su, T. L. Windus, M. Dupuis, and J. A. Montgomery, J. Comput. Chem. **14**, 1347 (1993).

[13] J. Andzelm, M. Klobukowski, E. Radzio-Andzelm, Y. Sakai, and H. Tatewaki, in *Gaussian Basis Sets for Molecular Calculations*, edited by S. Huzinaga (Elsevier, Amsterdam, 1984).

[14] T. H. Dunning, Jr., J. Chem. Phys. **90**, 1007 (1989).

[15] F. Jensen, J. Chem. Phys. **115**, 9113 (2001); **116**, 7372 (2002).

[16] A. D. Becke, J. Chem. Phys. **98**, 5648 (1993); C. Lee, W. Yang, and R. G. Parr, Phys. Rev. B **37**, 785 (1988); R. Colle and O. Salvetti, Theor. Chim. Acta **37**, 329 (1975).

[17] D. Vanderbilt, Phys. Rev. B **41**, 7892 (1990).

[18] H. J. Monkhorst and J. D. Pack, Phys. Rev. B **13**, 5188 (1976).

[19] MATERIALS STUDIO 4.4, http://www.accelrys.com

[20] S. J. Clark, M. D. Segall, C. J. Pickard, P. J. Hasnip, M. J. Probert, K. Refson, and M. C. Payne, Z. Kristallogr. **220**, 567 (2005).

[21] W. Kohn and L. J. Sham, Phys. Rev. **140**, A1133 (1965).

[22] Electron affinity is obtained as the opposite of the difference between total energies of a molecule having an extra electron and the neutral one. Table I always gives the charged molecule values in the row following the corresponding neutral values.

[23] M. A. Duncan, A. M. Knight, Y. Negishi, S. Nagao, Y. Nakamura, A. Kato, A. Nakajima, and K. Kaya, Chem. Phys. Lett. **309**, 49 (1999).

[24] Using values given by the fifth column of Table I we get:
$27.21\times[-922.1723-(-921.6516-0.4990)]$ eV $=-0.59$ eV
for coronene,
$27.21\times[-922.2300-(-921.6660-0.4990)]$ eV $=-1.77$ eV
for negatively charged coronene,
$27.21\times[-2068.9095-(-2068.3971-0.4990)]$ eV $=-0.36$ eV
for supercoronene, and
$27.21\times[-2068.9919-(-2068.4469-0.4990)]$ eV $=-1.25$ eV
for negatively charged supercoronene.

[25] G. Schaftenaar and J. H. Noordik, J. Comput.-Aided Mol. Des. **14**, 123 (2000).

[26] N. Park, M. Yoon, S. Berber, J. Ihm, E. Osawa, and D. Tomanek, Ref. 3.

[27] M. Gomberg, J. Am. Chem. Soc. **22**, 757 (1900).

[28] A better insight can be obtained from the figures shown in: http://webbook.nist.gov/cgi/cbook.cgi?ID=B823&Units=SI&Mask=8

[29] The fact that the π bands of graphene cross at only a pair of **k** points at the Dirac energy is most probably the origin of this kind of mixed soft localization.